Kinetics and Mechanism of Oxygen Transfer to Methyloxo(dithiolato)rhenium(V) Complexes

Gábor Lente and James H. Espenson*

Ames Laboratory and Department of Chemistry, Iowa State University of Science and Technology, Ames, Iowa 50011

Received February 11, 2000

The kinetics and mechanism of the reactions of the dimeric and monomeric methyloxo(dithiolato)rhenium(V) complexes $[(o\text{-}SC_6H_4CH_2S)Re(O)CH_3]_2$ and $[(o\text{-}SC_6H_4CH_2S)PyRe(O)CH_3]$ (Py = pyridine) with XO, sulfoxides, and pyridine *N*-oxides are studied. In these reactions, an oxygen atom from XO is transferred to rhenium, from which it later removed. A reaction scheme is proposed to interpret the kinetic data. This scheme features the formation of a monomeric (sulfoxide)- or (pyridine *N*-oxide)(dithiolato)methyloxorhenium(V) complex followed by its bimolecular oxidation in a rate-controlling step. Several sulfoxides (methyl, methyl phenyl, and substituted diphenyl) all react at similar rates. Activation parameters are determined for dimethyl sulfoxide and di-4-tolyl sulfoxide from temperature-dependent studies. The reactions with pyridine *N*-oxides show autocatalysis in which the catalyst is confirmed to be pyridine formed in the reactions.

Introduction

Methyltrioxorhenium(VII) (CH_3ReO_3, abbreviated as MTO) is an air- and water-stable compound. It is soluble in a large variety of solvents and catalyzes certain atom-transfer reactions[1−5] involving lower valent rhenium intermediates.[6,7] A kinetic study of the rhenium-catalyzed stereospecific desulfurization of thiiranes[8] focused our attention on methyloxo(dithiolato)rhenium(V) complexes, which were expected to provide further insight into the mechanism of MTO-catalyzed processes. MTO reacts with 2-(mercaptomethyl)thiophenol, H_2mtp, in toluene to give the sulfur-bridged dimer $[MeReO(mtp)]_2$, designated **D**,[9] whose structural formula is given in Scheme 1. It is known that **D** is monomerized by a variety of ligands, giving rise to a new family of related complexes, **M**−L.[10−12] Suitable oxygen-transfer agents convert **D** to MTO. The overall equation of this process is

$$\mathbf{D} + 4\mathrm{XO} = 2\mathrm{MTO} + 4\mathrm{X} + 2\mathrm{RS{-}SR} \qquad (1)$$

in which RS−SR represents the disulfide oxidation product of the dithiolate ligand. The structural formulas of the molecules appearing in eq 1 for the case in which XO is a pyridine *N*-oxide are given in Scheme 1. Certain intermediates suggested as a result of this study are also depicted. In this paper, detailed kinetic and mechanistic studies are reported for reaction 1 with XO = dialkyl sulfoxides and pyridine *N*-oxides.

Scheme 1

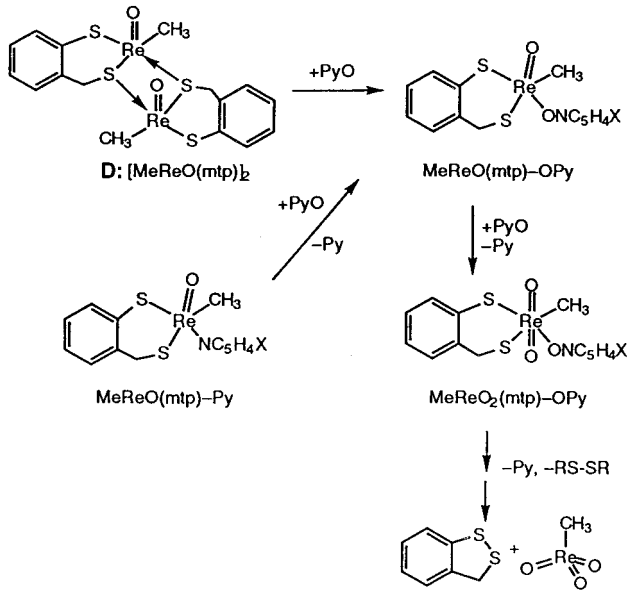

Experimental Section

Materials. MTO,[13] 2-(mercaptomethyl)thiophenol,[14,15] and dimer **D**[9] were synthesized as described. Other reagents were purchased from commercial sources and used without further purification. Benzene

(1) Romão, C. C.; Kühn, F. E.; Herrmann, W. A. *Chem. Rev.* **1997**, *97*, 3197−3246.
(2) Espenson, J. H.; Abu-Omar, M. M. *Adv. Chem. Ser.* **1997**, *253*, 99−134.
(3) Espenson, J. H. *Chem. Commun.* **1999**, 479−488.
(4) Conry, R. R.; Mayer, J. M. *Inorg. Chem.* **1990**, *29*, 4862−4867.
(5) Herrmann, W. A.; Romão, C. C.; Fischer, R. W.; Kiprof, P.; de Meric de Bellefon, C. *Angew. Chem., Int. Ed. Engl.* **1991**, *30*, 185−187.
(6) Abu-Omar, M. M.; Appelman, E. H.; Espenson, J. H. *Inorg. Chem.* **1996**, *35*, 7751−7757.
(7) Abu-Omar, M. M.; Espenson, J. H. *Inorg. Chem.* **1996**, *35*, 6239−6240.
(8) Jacob, J.; Espenson, J. H. *Chem. Commun.* **1999**, 1003.
(9) Jacob, J.; Guzei, I. A.; Espenson, J. H. *Inorg. Chem.* **1999**, *38*, 1040−1041.
(10) Jacob, J.; Lente, G.; Guzei, I. A.; Espenson, J. H. *Inorg. Chem.* **1999**, *38*, 3762−3763.
(11) Lente, G.; Jacob, J.; Guzei, I. A.; Espenson, J. H. *Inorg. React. Mech.*, in press.
(12) Lente, G.; Guzei, I. A.; Espenson, J. H. *Inorg. Chem.* **2000**, *39*, 1311−1319.
(13) Herrmann, W. A.; Kratzer, R. M.; Fischer, R. W. *Angew. Chem., Int. Ed. Engl.* **1997**, *36*, 2652−2654.
(14) Klingsberg, E.; Screiber, A. M. *J. Am. Chem. Soc.* **1962**, *84*, 2941−2944.
(15) Hortmann, A. G.; Aron, A. J.; Bhattacharya, A. K. *J. Org. Chem.* **1978**, *43*, 3374−3378.

10.1021/ic000148j CCC: $19.00
Published on Web 09/28/2000

(Fisher Spectranalyzed) was used as the solvent throughout this study. Unless otherwise stated, the rate constants reported herein were determined at 25.0 °C.

Instrumentation. Shimadzu scanning and diode-array spectrophotometers were used to record UV−vis spectra and kinetic curves. An Applied Photophysics DX-17 MV sequential stopped-flow apparatus was used in the single-mixing mode for fast reactions. The optical path length in the stopped-flow instrument was 1 cm. Standard calibration of the stopped-flow instrument gave the dead time as 1.26 ± 0.02 ms.[16] In every kinetics experiment, stopped-flow and conventional UV−vis, the measured initial absorbance was compared with that of a blank in which one of the reagents was absent to detect possible reactions occurring during the mixing time. Reactions were usually monitored in the 400−440 nm spectral region, where the brown intermediates (MeReO(mtp)−OX; X = Py, SR_2) of the oxygen-transfer reactions have intense absorptions (500−3000 L mol^{-1} cm^{-1}).

Computation. Stopped-flow curves were fitted with the nonlinear-least-squares routine in the software package provided by the manufacturer. Each observed rate constant was obtained as the average of at least five values determined from replicate kinetic runs and was reproducible within 5%. Rate constants from spectrophotometric experiments were obtained with nonlinear-least-squares fitting. Linearized forms were used only to visualize data.

Results

Preliminary Considerations. Reaction 1 was monitored by NMR spectroscopy with one or more resonances from every reagent being used to identify the products and confirm the stoichiometry. The only products detected were the ones shown in eq 1. Because the reactions were accompanied by considerable color changes, kinetics experiments were carried out by using UV−vis spectrophotometry, which is the more precise method. MTO, a product of reaction 1, is a well-known catalyst for oxygen transfer, and thus extra care was taken to detect possible autocatalytic effects during the kinetics experiments. In addition to compounds studied in this paper, arsine oxides, amine oxides, perchlorate, and periodate ions also oxidize **D** to MTO. No oxygen transfer was detected with phosphine oxides for thermodynamic reasons, because the P═O bond is stronger than any Re═O bond in this study. Likewise, dinitrogen oxide, epoxides, and sulfones failed to react, but now for kinetic reasons. Perhaps the bond to oxygen is not sufficiently polar to engage in coordination with rhenium to a sufficient extent.

Sulfoxides. The direct reaction of **D** with sulfoxides is very slow. Monomerization was shown to be rate controlling for the overall reaction[10,11]

$$[\mathrm{MeReO(mtp)}]_2 + 2\mathrm{R_2SO} \rightarrow 2\mathrm{MeReO(mtp)}{-}\mathrm{OSR_2} \quad (2)$$

Thus no kinetic information regarding oxygen transfer could be obtained. The monomeric pyridine complex **M**−Py reacted much more rapidly with sulfoxides and gave information on the oxygen-transfer step. Biphasic kinetics was observed. In the initial phase, the green color of **M**−Py became brown in a few seconds. This step was shown to be a ligand substitution, producing a monomeric sulfoxide complex. Detailed kinetic experiments for the first step were carried out using dimethyl sulfoxide:

$$\mathbf{M}{-}\mathrm{Py} + \mathrm{Me_2SO} \rightleftarrows \mathbf{M}{-}\mathrm{OSMe_2} + \mathrm{Py} \quad (3)$$

Figure 1 shows stopped-flow kinetic curves for the initial process ($\lambda = 475$ nm was found to be optimal for monitoring). As seen from comparison of these curves with that of the blank, there is no evidence to suggest that a reaction had occurred prior to or during the mixing time. The curves in Figure 1 also show that the process is inhibited by excess pyridine. Reaction 3 was confirmed to be an equilibrium and the following rate law was found:

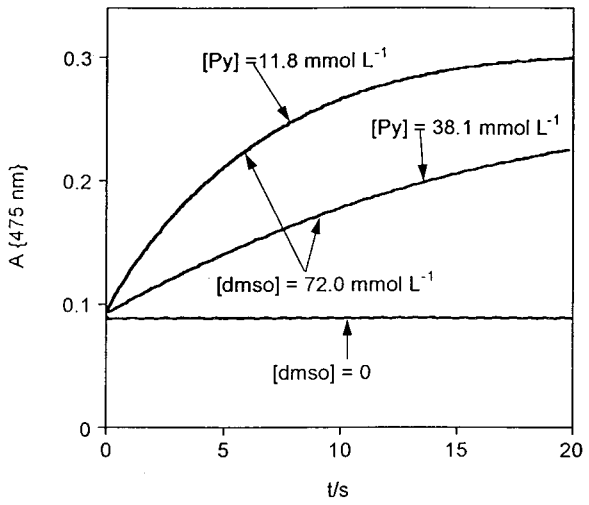

Figure 1. Sample stopped-flow kinetic curves for the initial part of the reaction between **M**−Py and dmso in benzene at 25 °C. $[\mathbf{M}{-}\mathrm{Py}]_0 = 0.598$ mmol L^{-1} for all curves.

$$\frac{\mathrm{d}[\mathbf{M}{-}\mathrm{OSMe_2}]}{\mathrm{d}t} = k_3\frac{[\mathbf{M}{-}\mathrm{Py}][\mathrm{Me_2SO}]}{[\mathrm{Py}]} - k_{-3}[\mathbf{M}{-}\mathrm{OSMe_2}] \quad (4)$$

The equilibrium constant for this process is defined as $K_3 = k_3/k_{-3}$ Thus the pseudo-first-order equilibration rate constant for the reaction is

$$k_{\mathrm{eq}} = k_3\frac{[\mathrm{Me_2SO}]}{[\mathrm{Py}]} + \frac{k_3}{K_3} \quad (5)$$

The parameters $k_3 = (1.84 \pm 0.03) \times 10^{-2}$ s^{-1} and $K_3 = 1.3 \pm 0.3$ were determined by least-squares fitting. These, in turn, give $k_{-3} = (1.4 \pm 0.3) \times 10^{-2}$ s^{-1}. The equilibrium constant (and thus the rate constant of the reverse reaction) could not be determined more precisely because this would have required the use of either lower dmso or higher pyridine concentrations, conditions under which the initial ligand substitution and the subsequent oxygen-transfer steps would no longer have been separated.

Figure 2 shows kinetic curves for the second step of the reaction. This process was carefully tested for autocatalysis with dmso. Prior addition of any of the products (MTO, the cyclic disulfide RS−SR, or dimethyl sulfide) did not influence the kinetic traces. The rate of the reaction was independent of the free dmso and pyridine concentrations when dmso was used in an excess sufficiently large to force the equilibrium of reaction 5 to give practically stoichiometric amounts of $\mathbf{M}{-}\mathrm{OSMe_2}$. A simple rate law was confirmed:

$$-\frac{\mathrm{d}[\mathbf{M}{-}\mathrm{OSMe_2}]}{\mathrm{d}t} = k_{\mathrm{SO}}[\mathbf{M}{-}\mathrm{OSMe_2}]^2 \quad (6)$$

The kinetic curves were fitted to an integrated second-order rate equation.[17] The value of k_{SO} can be calculated directly because the initial concentration of $\mathbf{M}{-}\mathrm{OSMe_2}$ is known. Values

(16) Tonomura, B.; Nakatani, H.; Ohnishi, M.; Yamaguchi-Ito, J.; Hiromi, K. *Anal. Biochem.* **1978**, *84*, 370−382.

(17) Espenson, J. H. *Chemical Kinetics and Reaction Mechanisms*, 2nd ed.; McGraw-Hill: New York, 1995; p 24.

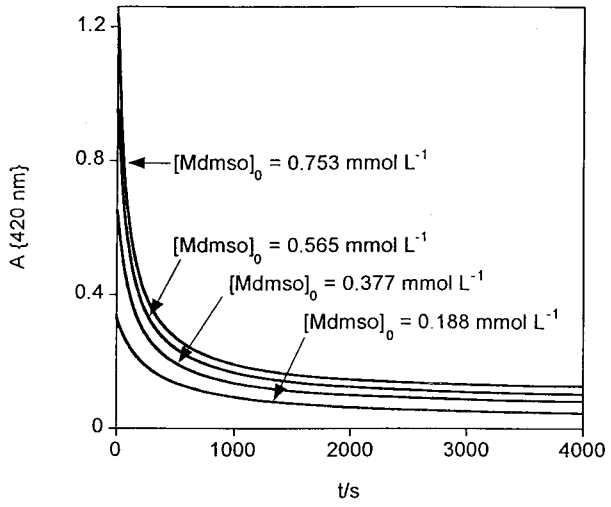

Figure 2. Sample kinetic curves for the oxygen-transfer step of the reaction between **M**−Py and dmso in benzene at 25.0 °C.

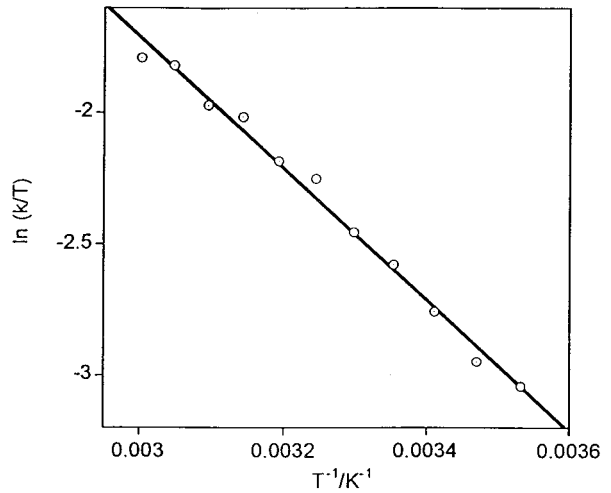

Figure 3. Eyring plot for the oxygen-transfer step of the reaction between **M**−Py and dmso in benzene.

Table 1. Rate Constants for the Oxygen-Transfer Steps of the Reactions between **M**−Py and Sulfoxides in Benzene at 25.0 °C

compound	k_{SO}/L mol^{-1} s^{-1}	compound	k_{SO}/L mol^{-1} s^{-1}
dimethyl sulfoxide	20.7 ± 0.6	bis(4-methoxyphenyl) sulfoxide	15.2 ± 0.2
methyl phenyl sulfoxide	15.8 ± 0.2	di-4-tolyl sulfoxide	21.3 ± 0.2
diphenyl sulfoxide	18.8 ± 0.4	bis(4-chlorophenyl) sulfoxide	22.2 ± 0.5

of the k_{SO} rate constants with various sulfoxides are summarized in Table 1. It can be seen that the second-order rate constants are almost independent of the identity of the sulfoxide.

Figure 3 shows the evaluation of the temperature dependence of k_{SO} for the reaction with dmso over the range 10−60 °C. The activation parameters were determined as $\Delta H^{\ddagger} = 20.8 \pm 0.7$ kJ mol^{-1} and $\Delta S^{\ddagger} = -149 \pm 2$ J K^{-1} mol^{-1}. Another series of measurements on bis(4-methylphenyl) sulfoxide at 8−60 °C gave $\Delta H^{\ddagger} = 17 \pm 2$ kJ mol^{-1} and $\Delta S^{\ddagger} = -165 \pm 5$ J K^{-1} mol^{-1}.

To obtain further evidence for the mechanism, the reaction between the monomeric 4-methylpyridine complex, **M**−4-MeC$_5$H$_4$N and dmso was also studied. The product of the initial ligand substitution step gave the same UV spectrum (Figure 14 in the Supporting Information) as the one using **M**−Py; the second-order rate constant determined from the oxygen-transfer step was the same as with **M**−Py. These findings indicate that the same (pyridine-free) intermediate is formed in the two reactions and give further support to our interpretation.

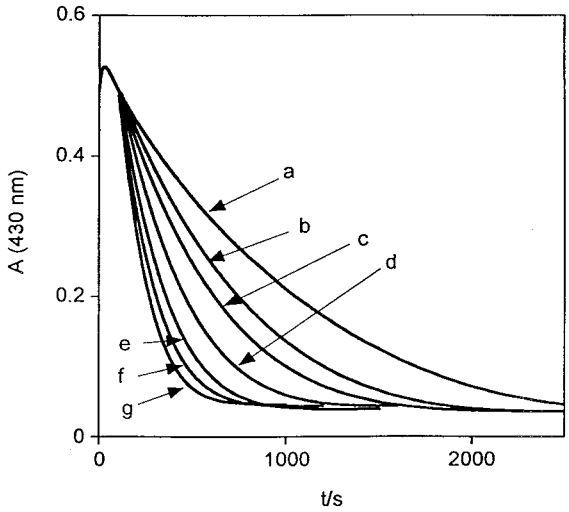

Figure 4. Kinetic curves demonstrating autocatalysis in the reaction of **D** with 4-methylpyridine *N*-oxide in benzene at 25.0 °C. 4-Methylpyridine was added at 90 s during each kinetic run except (a). Initial concentrations: [**D**] = 0.200 mmol L^{-1} and [4-MePyO] = 39.7 mmol L^{-1} for all curves; [4-MePy] = 0 (a), 3.7 (b), 7.3 (c), 14.7 (d), 22.0 (e), 29.3 (f), 36.6 (g) mmol L^{-1} after the addition.

Pyridine *N*-Oxides. The direct reaction of **D** with pyridine *N*-oxides (PyO) was reasonably fast and showed biphasic kinetics. The first step was the formation of brown monomeric pyridine *N*-oxide complexes in a few seconds:

$$\mathbf{D} + 2\mathrm{PyO} \rightarrow 2\mathbf{M}{-}\mathrm{OPy} \qquad (7)$$

The kinetics of this monomerization step with 4-methylpyridine *N*-oxide was reported earlier.[12] The second step was separated in time from the first and was confirmed to be the oxygen-transfer stage. A detailed kinetic study was undertaken with 4-methylpyridine *N*-oxide, the most benzene-soluble of the compounds used.

An initial-rate study (Figures 7 and 8 in the Supporting Information) of the oxygen-transfer step showed that the reaction was first-order with respect to both the monomeric pyridine *N*-oxide complex and free pyridine *N*-oxide. The rate equation from the initial-rate analysis is

$$v_i = k_{PyO}[\mathbf{M}{-}\mathrm{OPy}][\mathrm{PyO}] \qquad (8)$$

The value $k_{PyO} = 0.0240 \pm 0.0015$ L mol^{-1} s^{-1} was determined from the initial rates. However, this rate equation could not be used to describe full kinetic curves, which were slightly autocatalytic. Midcourse addition of one of the products, 4-methylpyridine (Py), accelerated the reaction as shown in Figure 4. Prior addition of MTO did not influence the kinetic curves (Figure 10 in the Supporting Information).

When 4-methylpyridine was added midcourse in a large excess over Re, pseudo-first-order kinetic curves were obtained. A kinetic analysis of these curves revealed a first-order dependence on the concentration of pyridine for the catalytic pathway (Figures 11 and 12 in the Supporting Information). Thus, the full rate equation is

$$-\frac{\mathrm{d}[\mathbf{M}{-}\mathrm{OPy}]}{\mathrm{d}t} = (k_{PyO}[\mathrm{PyO}] + k_{Py}[\mathrm{Py}])[\mathbf{M}{-}\mathrm{OPy}] \qquad (9)$$

Table 2. Rate Constants Determined with Substituted Pyridine *N*-Oxides in Benzene at 25.0 °C

compound	k_{PyO}/L mol^{-1} s^{-1}	compound	k_{PyO}/L mol^{-1} s^{-1}
4-methylpyridine *N*-oxide	$(2.40 \pm 0.15) \times 10^{-2}$	4-cyanopyridine *N*-oxide	$(3.5 \pm 0.4) \times 10^{-2}$
pyridine *N*-oxide	$(1.97 \pm 0.09) \times 10^{-2}$	4-nitropyridine *N*-oxide	$\sim 1 \times 10^{-2}$

With the value of k_{PyO} fixed at 2.4×10^{-2} L mol^{-1} s^{-1}, least-squares fitting gave $k_{Py} = 0.153 \pm 0.004$ L mol^{-1} s^{-1}. Numerical integration based on this rate equation[18] gave a reasonable fit to the curves that had been measured without the addition of 4-methylpyridine.

In the experiments described in the previous paragraph, 4-methylpyridine was added midcourse and not at the start because pyridines react with **D**, giving monomeric **M**−Py complexes.[11] Prior addition of pyridine would complicate the initial speciation of rhenium. In the midcourse addition experiments, a comparison of the UV−vis spectra obtained immediately (∼3−4 s) before and after the addition of 4-MePy revealed no significant spectral changes, which showed that the speciation of rhenium did not change.

Reverse mixing experiments were also performed. Experiments using **M**−4-MePy as a starting complex were also carried out with 4-methylpyridine *N*-oxide. Spectrophotometric detection showed that this reaction, after a fast ligand substitution process, gave the same **M**−OPy intermediate as was detected in the reaction of **D** with 4-methylpyridine *N*-oxide (Figure 13 in the Supporting Information). The kinetics of the subsequent oxygen-transfer step was in good agreement with results from previous experiments using **D** as the initial rhenium(V) complex. The k_{PyO} rate constants determined from the initial parts of the kinetic curves with several substituted pyridine *N*-oxides are presented in Table 2.

Discussion

The Ligand Substitution Step. The mechanism for the ligand substitution reaction, eq 3, requires attention because it is unique. This reaction is, in a stoichiometric sense, like all reactions between MeReO(mtp)X and an entering ligand Y, a considerable number of which have recently been reported.[11,12] With X = Py and Y = R_2SO, the data show that the equilibrium concentrations are consistent with eq 3 being the proper equation for the net reaction. The kinetic data, however, are unusual. In all of the many previous cases, the reaction rates in both directions were found to be directly proportional to the concentrations of the ligands entering from those directions. With X = Py and Y = R_2SO, the forward reaction has an inverse dependence on the pyridine concentration; the reverse reaction is pyridine independent. A formal reaction scheme for this special case, X = Py and Y = R_2SO, can be diagrammed as follows:

$$\mathbf{M}\text{−Py} + R_2SO \underset{k_{-a}}{\overset{k_a}{\rightleftharpoons}} \text{Int} + \text{Py}; \quad \text{Int} \underset{k_{-b}}{\overset{k_b}{\rightleftharpoons}} \mathbf{M}\text{−OSR}_2 \qquad (10)$$

If the first reaction occurs much more rapidly than the second,[19] the rate law then agrees with the experimental form

$$v = \frac{k_a k_b[\mathbf{M}\text{−Py}][R_2SO]}{k_{-a}[\text{Py}]} - k_{-b}[\mathbf{M}\text{−OSR}_2] \qquad (11)$$

In this analysis, the intermediate does not attain a concentration high enough for detection. The derived rate equation has the same form as the experimental equation. The chemical sense of the mechanism is that the "ordinary" bimolecular substitution, the first step in eq 10, occurs rapidly relative to a second step that is unique to this ligand combination. The second step may be no more than a linkage isomerization, $\mathbf{M}\text{−S(O)R}_2 \rightarrow \mathbf{M}\text{−OSR}_2$. Or the intermediate might instead be an end-on $\mathbf{M}\text{−OSR}_2$ species, leading to side-on Me_2SO, analogous to the well-known peroxo complex of MTO[3,20] but apparently without precedent in any structurally characterized material. We cannot argue the structure of the reactive transient any further, for it never builds up to a level detectable by spectroscopy.

An alternative explanation for the kinetics of reaction 3 is given by the scheme

$$\mathbf{M}\text{−Py} \underset{k_{-c}}{\overset{k_c}{\rightleftharpoons}} \mathbf{M} + \text{Py}; \quad \mathbf{M} + R_2SO \underset{k_{-d}}{\overset{k_d}{\rightleftharpoons}} \mathbf{M}\text{−OSR}_2 \qquad (12)$$

Again, with the first reaction much faster than the second, the derived rate law is

$$v = \frac{k_c k_d[\mathbf{M}\text{−Py}][R_2SO]}{k_{-c}[\text{Py}]} - k_{-d}[\mathbf{M}\text{−OSR}_2] \qquad (13)$$

Although it is correct mathematically, we are inclined to discount this alternative on the basis of certain considerations. In none of the other cases is there any indication of a dissociative component to the mechanism, like that shown in the first step of eq 12, in which the "bare monomer" **M** occurs as an intermediate. The rate equations of ligand substitution processes studied earlier, which were found to adopt an associative (I_a) mechanism, and the role of the putative **M** were found to be unimportant.[12] The process is also much slower than one would expect on the basis of the rate of pyridine exchange on **M**−Py.[12] Finally, to attain eq 11, $k_{-c}[\text{Py}] \gg k_d[R_2SO]$ would be required at all concentrations. These considerations lead us to support the two-step reaction scheme in eq 10, which involves a bond isomerization rather than a dissociative process.

Oxygen Atom Transfer Involving PyO Species. Scheme 1 shows the mechanism that we are proposing for the oxygen-transfer reactions of the pyridine *N*-oxides described in this paper. The rate-controlling step for oxygen transfer is the bimolecular oxidation of **M**−OPy by the oxidizing agent PyO. It is only plausible, however, that this transformation occurs in (at least) two steps, the first and faster being coordination of the Lewis base PyO to the vacant (sixth) coordination site on rhenium. The rate-controlling process is then the breaking of the covalent oxygen−nitrogen bond. As it stands, this important step is closely linked with the two coordination equilibria preceding it, which makes it difficult to isolate the reaction of interest in this system. Reactions with substituted pyridine *N*-oxides show little variation in the rate constants of the rate-controlling steps. These rate constants fall within a factor of 4 for the derivatives studied, and no particular pattern in the variation can be seen.

The resulting rhenium compound is $MeRe(O)_2(mtp)$ or $MeRe(O)_2(mtp)OPy$, a dioxorhenium(VII) compound. Evidence for it in this system is entirely circumstantial, as it has but a fleeting

(18) Peintler, G. Ph.D. Thesis, Attila József University, Szeged, Hungary, 1997.

(19) Literally, this is not possible because all the steps of a steady-state sequence proceed at the same rate. This usage is casual but common (and harmless); here it means that $(k_a[\text{Y}] + k_{-a}[\text{X}]) \gg (k_b + k_{-b}[\text{Y}])$.

(20) Herrmann, W. A.; Fischer, R. W.; Scherer, W.; Rauch, M. U. *Angew. Chem., Int. Ed. Engl.* **1993**, *32*, 1157−1160.

existence under these conditions; however, in other reactions, it can be trapped by, for instance, triphenylphosphine:[21]

$$MeRe(O)_2(mtp) + PPh_3 \rightarrow MeReO(mtp) + Ph_3P{=}O \quad (14)$$

We have also learned that, if the trapping reaction is made less efficient (by choice of the phosphine or its concentration), trapping then competes with reductive elimination of the disulfide. The latter is the step that we propose to be the final one in this reaction, in that both $MeReO_3$ and the disulfide of mtp are products. An equation for this reaction, which itself is likely a composite of more than one step, can be given by

$$MeRe(O)_2(mtp)OPy \rightarrow MeReO_3 + RS{-}SR + Py \quad (15)$$

Oxidation by Sulfoxides. There is a quite noticeable distinction between the pyridine *N*-oxide and sulfoxide reactions. The kinetics describe, in one case, a reaction between **M**−OPy and PyO and, in the other, a reaction between two **M**−OSR_2 species. The latter case requires a reaction between two monomeric **M**−OSR_2 molecules that leads to the expulsion of one R_2S molecule. A sulfoxide bonded to rhenium is a much better oxidizing agent than a free sulfoxide, owing to the strength of the resulting Re=O bond. The immediate product of the rate-controlling step is a methyldioxo(dithiolato)rhenium(VII) complex, likely $MeRe(O)_2(mtp)-OSR_2$, which subsequently expels a molecule of cyclic disulfide and a molecule of R_2S, analogous to the reaction represented by eq 15. It should be noted that the seemingly feasible unimolecular decomposition of **M**−OX to a dioxorhenium(VII) species and R_2S seems to be unimportant in that all the rate-controlling steps were clearly second-order reactions.

The rate constants (Table 1) vary little among the sulfoxides. As shown with two examples, the oxygen-transfer reaction with sulfoxides has a low enthalpy of activation and a substantially negative entropy of activation. These parameters reflect the finding that the second-order rate constants for dmso increase by only a factor of 4 over the range 10−60 °C. The low enthalpy of activation gives some further support to our structural proposal for dmso in that the sulfur−oxygen double bond is but partially broken; also, however, the experimental value of $\Delta H^{\ddagger}$ may be much smaller than that of the rate-controlling step, being in part offset by $\Delta H°$ from the two preceding equilibrium steps.

Electronic effects were studied with substituted diphenyl sulfoxides. A Hammett correlation plot (Figure 15 in the Supporting Information) gave a reaction constant of $\rho = 0.13 \pm 0.08$, indicating the practical absence of electronic effects. This is expected because electronic effects are expected to influence the enthalpy of activation at a stage that is not dominant in the oxygen-transfer reaction. It should be also noted that dimethyl, methyl phenyl, and diphenyl sulfoxides have very similar rate constants. From this one might conclude that the organic groups on sulfur have little effect on the rate of reaction in general.

The Oxidation Step. Release of R_2S or pyridine in the rate-controlling step is accompanied by (more likely occasioned by) transfer of an electron pair from the metal:

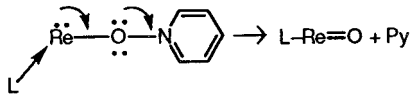

(21) Wang, Y.; Espenson, J. H. Unpublished observations.

The "extra ligand" on rhenium, whose presence in the transition state was documented by the kinetics, may be PyO, or it may be Py if the complex concentration is sufficiently high. The necessary function of one ligand or the other, as defined by the kinetics, is to donate electron density to the rhenium atom to effect the transformation shown.

With sulfoxides, the extra ligand is not R_2SO itself. Rather, a sulfoxide coordinated to rhenium is involved. There is really no factual basis for presenting the structure of this transition state; a purely conjectural hypothesis is offered solely to show that a reasonable postulate might be made. The structure of **D** in Scheme 1 shows that the sulfur atoms of the bidentate thiolate can make a bridge to a second rhenium. In this stable compound, the Re−S distances are barely distinct from one another: 229.9 pm (nonbridging Re−S), 236.2 pm (covalent Re−S in diamond core), and 238.6 pm (coordinate Re−S in diamond core). Thus, considerable electron donation to rhenium from a sulfur atom chelated to the other rhenium is suggested. This situation indicates that a plausible transition state exists, but it does not prove it. That remains for further work.

Catalysis with Pyridine. An interesting feature of the reaction with pyridine *N*-oxides is the autocatalytic nature of the process. The determined value of k_X for 4-methylpyridine *N*-oxide implies that the pyridine-catalyzed pathway plays a minor, although not negligible, role at the end of the reaction without extra pyridine added. There are two possible pathways for this catalytic effect, both of which are in agreement with the confirmed rate law. The first is that small amounts of **M**−4-MePy are formed in an equilibrium between **M**−OX and 4-MePy and that **M**−4-MePy is oxidized by XO much more rapidly than by **M**−OX. This possibility is unlikely, because no signs of the direct oxidation of **M**−4-MePy by OX were found independently. No analogous reaction between **M**−$OSMe_2$ and **M**−Py was detected, either. The second and preferred possibility is that **M**−OX and 4-MePy form small amounts of a six-coordinate rhenium(V) complex, XO−**M**−4-MePy, which, unlike the five-coordinate **M**−OX complex, has a unimolecular redox decomposition pathway that accounts for the catalytic process. The chemical equation is

$$MeReO(mtp)(OPy)Py \rightarrow MeRe(O)_2(mtp)Py + Py \quad (16)$$

In an earlier study, MTO was shown to form complexes with pyridines and pyridine *N*-oxides.[22] This complexation caused no complication for our kinetic studies, as pyridine *N*-oxides were used in large excess over Re; therefore the change in the concentration of free pyridine *N*-oxide was negligible. No kinetic role for the pyridine or pyridine *N*-oxide complexes of MTO could be found.

D, originally prepared from 2-(mercaptomethyl)thiophenol and MTO,[9] is then oxidized back to MTO in these oxygen-transfer reactions. Thus, one can envision a reaction between 2-(mercaptomethyl)thiophenol and an oxygen-transfer agent that is catalyzed by rhenium:

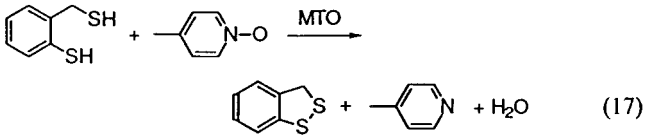

(17)

This reaction was confirmed experimentally. However, no

(22) Wang, W. D.; Espenson, J. H. *J. Am. Chem. Soc.* **1998**, *120*, 11335−11341.

kinetic study was undertaken because the mechanism for the formation of **D** still needs to be explored.

Acknowledgment. This research was supported by the U.S. Department of Energy, Office of Basic Energy Sciences, Division of Chemical Sciences, under Contract W-7405-Eng-82. G.L. also wishes to thank the U.S.-Hungary Science and Technology Program for financial support.

Supporting Information Available: Figures 5−17, showing spectral curves and plots of kinetic data to illustrate agreement with selected mathematical forms and to evaluate numerical parameters. This material is available free of charge via the Internet at http://pubs.acs.org.

IC000148J